

Article

Assessment of Changes in Key Ecosystem Factors and Water Conservation with Remote Sensing in the Zoige

Peng Hou¹, Jun Zhai^{1,*} , Dian-Dian Jin^{1,*}, Yan Zhou², Yan Chen¹ and Hai-Feng Gao¹

¹ Satellite Application Center for Ecology and Environment, Ministry of Ecology and Environment of People's Republic of China, Beijing 100094, China; houpcy@163.com (P.H.); chenyan30033@163.com (Y.C.); gaohf03@hotmail.com (H.-F.G.)

² Ministry of Education Key Laboratory of Geospatial Technology for the Middle and Lower Yellow River Regions, Henan University, Kaifeng 475004, China; yanzhou152@126.com

* Correspondence: zhajj@lreis.ac.cn (J.Z.); jin_diandian@163.com (D.-D.J.)

Abstract: As the largest alpine peat swamp wetland distribution area in the world, the Zoige has important ecological functions, including water conservation and biodiversity maintenance. In the past 20 years, the regional ecological protection and restoration measures continuously strengthened under the leadership of the local government have led to gradual improvements in the ecological environment of the region. In this study, multisource satellite remote-sensing image data were used to carry out quantitative monitoring and assessment of the main ecological elements (vegetation and water), as well as the regional leading ecosystem service function in the Zoige. Combined with local ecological protection management policies and measures, we analyzed the characteristics and effectiveness of ecological protection. We compared the ecosystem change trends of the Zoige reserve and the county, from 2001 to 2020, and found that the fractional vegetation cover (FVC) of Zoige county has increased at a rate of 0.25%/year. The growth rate was highest between 2015 and 2020, and the growth rate of FVC in the Zoige Wetland National Nature Reserve is approximately 1.89-fold that of the whole county. The water area also shows similar variation characteristics. On the whole, the water conservation capacity of the Zoige showed a significant increase from 2001 to 2020. We used high-resolution satellite remote-sensing images to capture the details of land use changes brought about by local ecological protection policies and measures, and together with macroecological indicators, we reflected on the effectiveness of regional ecological protection measures. We observed that the ecological effects of nature reserves are more direct and rapid, and the amount of water conservation within the nature reserve is about $1 \times 10^4 \text{ m}^3/\text{km}^2$ higher than that of the surrounding grasslands. Satellite remote-sensing images can not only capture the multiscale change information of ecological indicators, such as vegetation and water, in a timely manner, but can also help us to identify the effectiveness of conservation measures by distinguishing and analyzing the causes of these changes.

Keywords: Zoige wetland; nature reserve; fractional vegetation cover; water conservation; ecological conservation



Citation: Hou, P.; Zhai, J.; Jin, D.-D.; Zhou, Y.; Chen, Y.; Gao, H.-F. Assessment of Changes in Key Ecosystem Factors and Water Conservation with Remote Sensing in the Zoige. *Diversity* **2022**, *14*, 552. <https://doi.org/10.3390/d14070552>

Academic Editor: Corrado Battisti

Received: 5 June 2022

Accepted: 6 July 2022

Published: 9 July 2022

Publisher's Note: MDPI stays neutral with regard to jurisdictional claims in published maps and institutional affiliations.



Copyright: © 2022 by the authors. Licensee MDPI, Basel, Switzerland. This article is an open access article distributed under the terms and conditions of the Creative Commons Attribution (CC BY) license (<https://creativecommons.org/licenses/by/4.0/>).

1. Introduction

Wetlands represent the transitional zone between terrestrial and aquatic ecosystems, and possess a unique ecosystem and functional characteristics [1,2]. At present, changes in vegetation and water bodies are basic factors that reflect the status of and changes in wetland ecosystems, and are key indicators of wetland shrinkage and restoration monitoring based on satellite remote sensing [3,4].

The Zoige wetland is located on the eastern edge of the Qinghai Tibet Plateau and is listed as an “International Important Wetland” by UNESCO [5,6]. It is an important water conservation area in the upper reaches of the Yellow and Yangtze Rivers, with the

largest plateau peat swamp in the world [7]. It is a key area for biodiversity protection both in China and worldwide [8]; it is also an important habitat for wildlife species, such as the black-necked cranes and white-tailed sea eagles, and is highly sensitive to climate change [9,10]. The Zoige Wetland National Nature Reserve was established in 1998 and covers an area of 1665.70 km². The alpine swamp wetland ecosystems, black-necked cranes, and other rare animals are especially targeted for protective measures.

Owing to the joint impact of climate change and human activities, the Zoige wetland has been shrinking since the 1950s, resulting in the decline in the groundwater level, land degradation, reduction in biodiversity, and increased carbon emissions. Relevant research has mainly focused on regional climate change analysis [11–13], wetland area change monitoring [14], grassland degradation, land desertification [15–17], soil organic carbon change [18,19], and ecosystem services and health [20,21]. Most of these studies were published before 2016, and the conclusions were mainly based on the continuous degradation of the ecological environment. There is still a lack of analysis on the effectiveness of conservation measures.

Since the 1970s, China has successively launched a series of ecological protection and restoration projects, including the Natural Forest Protect Projection, the Grain for Green program, and the Returning Rangeland to Grassland, which have increased regional ecological functions [22,23]. Since 2003, ecological protection and restoration projects, such as grassland restoration and desertification land management, have significantly increased in the Zoige area [24–26], and a series of restoration and rectification works of nature reserves have been carried out in succession. In the past 30 years, the growth rate of regional desertification land has significantly slowed [17,25]. The project of returning grazing land to grassland in the county has had significant benefits: the vegetation height in the project area has elevated by 69.1% on average, compared with that in the nonproject area [26].

From the perspective of satellite remote sensing, we used the main elements of the ecosystem (vegetation, water bodies, etc.) and the service function of water conservation, as indicators to analyze the changing characteristics of the ecological environment in Zoige county and nature reserves [27]. Simultaneously, combined with high-resolution remote-sensing images and field investigations, we attempted to link the direct image evidence of ecological restoration with the above-mentioned remote-sensing indicators of ecological change, thus further elaborating the obvious ecological benefits brought about by ecological protection and supervision.

2. Materials and Methods

2.1. Study Area

Zoige county (102°08–103°39' E, 32°56–34° N) is located in the northern part of the Northwest Sichuan Plateau, which is the core area of the Zoige wetland. The topography is low in the middle and high in the surrounding areas. It belongs to the Aba Tibetan and Qiang Autonomous Prefecture of Sichuan province, and has a total area of 1.04×10^4 km² and an average altitude of 3471 m (Figure 1). The regional altitude difference is largely attributed to the depth of the river. The study area has a plateau cold temperate humid monsoon climate, with an annual average temperature of 1.1 °C, and annual precipitation of 650 mm [28]. However, in recent years, there has been an obvious trend of warming and drying [29].

2.2. Vegetation Data Acquisition and Calculation Method

Fractional vegetation cover (FVC) reflects the vegetation coverage of a certain area, and is an important indicator for measuring the quality of vegetation and ecosystem change [30]. Based on the remote-sensing cloud platform of Google Earth Engine and the Moderate Resolution Imaging Spectroradiometer (MODIS) 13Q1 normalized difference vegetation index (NDVI) product (<https://ladsweb.modaps.eosdis.nasa.gov>, (accessed on 5 June 2021)), we used the pixel dichotomy model to calculate the vegetation coverage [31,32]. The MODIS

13Q1 NDVI product has a temporal resolution of 16 days with 23 cycles of data per year. In this study, FVC data for 23 periods were generated annually, and then aggregated into the average annual FVC. The specific formula of FVC is as follows:

$$FVC = \frac{NDVI - NDVI_s}{NDVI_v - NDVI_s} \quad (1)$$

where $NDVI_v$ and $NDVI_s$ are the NDVI pixel values of pure vegetation and bare land, respectively. With the NDVI value statistics, we determined the cumulative frequency of 1% $NDVI_s$ and cumulative frequency of 99% $NDVI_v$ [33].

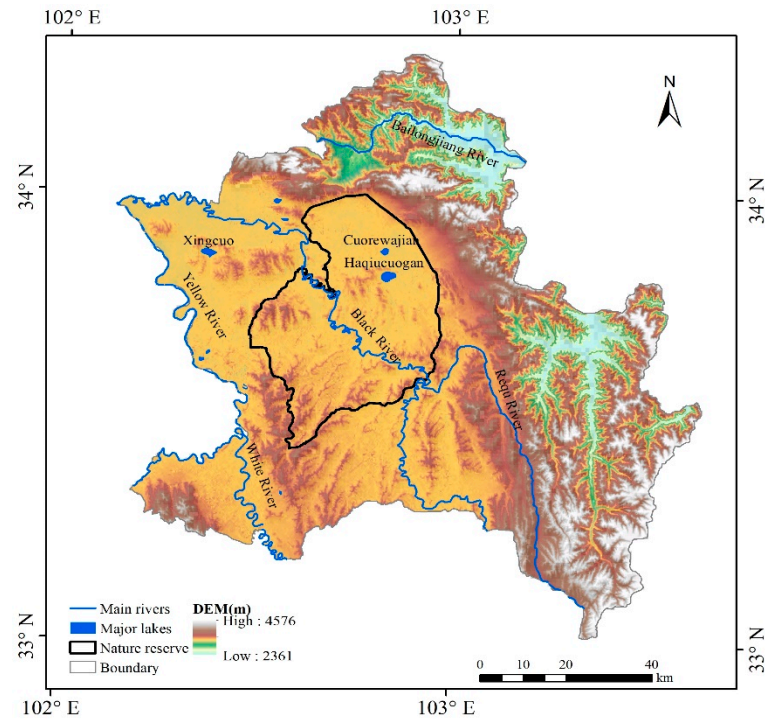


Figure 1. Topographical map of Zoige County.

2.3. Water Data and Acquisition Methods

Water information in this study mainly included open water surfaces, such as rivers and lakes. Using information based on the Google Earth Engine platform, long time-series Landsat remote-sensing image data (<https://landsweb.modaps.eosdis.nasa.gov>, (accessed on 24 May 2021)) corresponding to the study area and study period were directly called through the database, from which the vegetation, water, and dry naked index were calculated [34]. Each index is calculated as follows:

$$NDVI = \frac{\rho_{NIR} - \rho_{red}}{\rho_{NIR} + \rho_{red}} \quad (2)$$

$$MNDWI = \frac{\rho_{Green} - \rho_{SWIR}}{\rho_{Green} + \rho_{SWIR}} \quad (3)$$

$$AWEI = \rho_{Blue} + 2.5 \times \rho_{Green} - 1.5 \times (\rho_{NIR} + \rho_{SWIR1}) - 0.25 \times \rho_{SWIR2} \quad (4)$$

$$DBSI = \frac{\rho_{SWIR1} - \rho_{Green}}{\rho_{SWIR1} + \rho_{Green}} - NDVI \quad (5)$$

where $NDVI$ is the normalized vegetation index, $MNDWI$ is the improved normalized difference water body index, $AWEI$ is the automatic water body extraction index, $DBSI$ is the dry bare index, ρ_{Blue} is the blue band, ρ_{Green} is the green band, ρ_{NIR} is the near-infrared

band, ρ_{red} is the red band, ρ_{SWIR1} is the short-wave infrared band 1, and ρ_{SWIR2} is the short-wave infrared band 2.

Secondly, the regional water body area was extracted by combining the remote-sensing water body index and the basin relative elevation setting, and the non-water-body information was filtered by combining the vegetation index and drought exposure index [34]. Among them, 30 m spatial resolution digital elevation model (DEM) products came from the geospatial data cloud platform (<http://www.gscloud.cn>, (accessed on 24 May 2021)).

Finally, the annual data product of flood frequency (the ratio of the number of times a place is submerged to the number of effective observation) was constructed using annual multiperiod water body data to determine the flood frequency [34,35]. Then, the human-computer interaction method was used to determine the data threshold of flooding frequency, which could maximize the avoidance of seasonal water and noise (the threshold in the study is 70%), and obtain the stable water distribution of the study area in the current year.

2.4. Ecosystem Function Assessment

Water conservation means that ecosystems (such as forests, grassland, etc.) intercept infiltrate, accumulate precipitation through their unique structures and water interactions, and control water flow and the water cycle through evapotranspiration. We used the water balance equation to calculate water conservation capacity [36]:

$$TQ = \sum_{i=1}^j (P_i - R_i - ET_i) \times A_i \times 10^3 \quad (6)$$

where TQ is water conservation (m^3), P_i is rainfall (mm), R_i is surface runoff (mm), ET_i is evapotranspiration (mm), A_i is the type i ecosystem area (km^2), i is the type i ecosystem in the study area, and j is the number of ecosystem types in the study area.

Rainfall data were obtained from a TerraClimate dataset with a spatial resolution of 1 km (<https://climate.northwestknowledge.net/TERRACLIMATE/index>, (accessed on 10 June 2021)). Evapotranspiration data were the result of the MODIS MOD16A3 product, with a spatial resolution of 1 km (<https://ladsweb.modaps.eosdis.nasa.gov>, (accessed on 24 June 2021)). The surface runoff was obtained by multiplying the rainfall by the surface runoff coefficient, and the surface runoff coefficient was obtained from the literature [36]. The ecosystem area was derived from data comprising remote-sensing surveys and assessments of the national ecological status, which mainly included forest, shrub, grassland, garden, and wetland types [37].

To avoid the influence of the interannual precipitation fluctuations, based on the calculation of annual water conservation, we took the average every five years to represent the regional water conservation capacity in different periods. Then, we comprehensively analyzed the change characteristics of water conservation function over the past 20 years.

2.5. Change Trend Analysis Method

For trend analysis, we used the Theil–Sen median method, a trend analysis method for nonparametric statistics. The calculation method of the Sen trend degree is as follows [38]:

$$\beta = \text{mean} \left(\frac{x_j - x_i}{j - i} \right), \forall j > i \quad (7)$$

where x_j and x_i are time series data, a β greater than 0 indicates an increasing trend in the time series, and a β of less than 0 indicates a decreasing trend in the time series.

The Mann–Kendall trend test is a nonparametric statistical test method for which measured values do not need to follow a normal distribution. The trend is not required

to be linear, and is not affected by missing values and outliers [39,40]. The statistical test method used is as follows:

$$Z_c = \begin{cases} \frac{S-1}{\sqrt{Var(s)}} & S > 0 \\ 0 & S = 0 \\ \frac{S+1}{\sqrt{Var(s)}} & S < 0 \end{cases} \quad (8)$$

$$S = \sum_{i=1}^{n-1} \sum_{j=i+1}^n sgn(x_j - x_i) \quad (9)$$

$$sgn(x_j - x_i) = \begin{cases} 1 & x_j - x_i > 0 \\ 0 & x_j - x_i = 0 \\ -1 & x_j - x_i < 0 \end{cases} \quad (10)$$

$$Var(s) = \frac{n(n-1)(2n+5)}{8} \quad (11)$$

where *sgn* is a symbolic function, x_j and x_i are sequential data sets, and n is the length of the data samples. Z_c followed a standard normal distribution. If $Z_c > Z_{(1-\alpha)/2}$, there is a significant trend change. $Z_{(1-\alpha)/2}$ is the corresponding value of the standard normal function distribution table at confidence level α . The confidence level α was set at 0.05.

3. Results

3.1. Vegetation Change Characteristics

The spatial distribution of fractional vegetation cover in Zoige county is shown in Figure 2. The FVC of the county in 2020 was 57.56%. Areas with large FVC (>70%) were mainly distributed in the eastern Zoige forest ecosystem, while areas of low FVC (<20%) were distributed in the northwest of the county where sandy, urban, and rural land were concentrated.

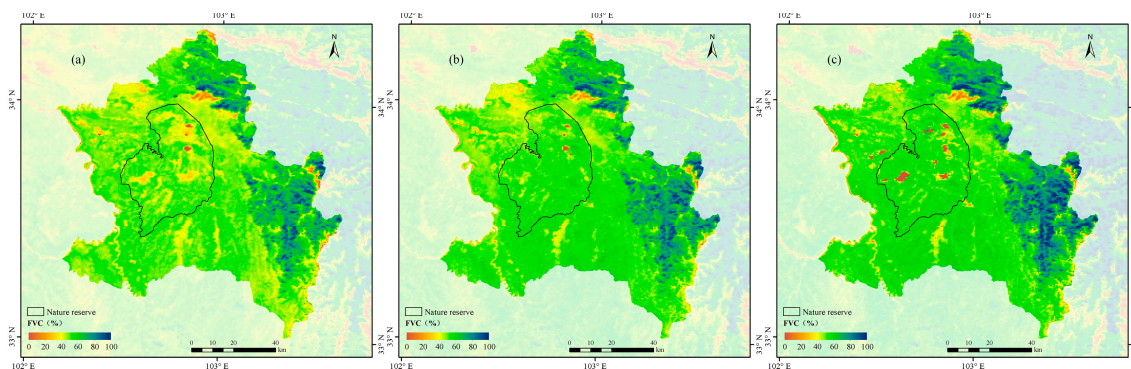


Figure 2. Spatial distribution of fractional vegetation cover (FVC) in Zoige in (a) 2001, (b) 2010, and (c) 2020.

In 2020, the average FVC of the nature reserve was 53.22%. Because the terrain was relatively flat, the grassland in the area was evenly distributed. Although the average vegetation coverage in the nature reserve was 4% lower than that of the whole county, the vegetation coverage of grassland ecosystems inside the reserve was 1% higher than that outside of the reserve.

Between 2001 and 2020, the FVC in Zoige demonstrated an overall upward trend, with an increase of 5.38% in 2020 compared with 2001. In particular, the rate of increase from 2015 to 2020 was significant compared with previous years (an increase of 1.35%). The average annual increase in FVC in this period was approximately 1.64-fold higher than that of the previous 15 years (2001–2015; Figure 3).

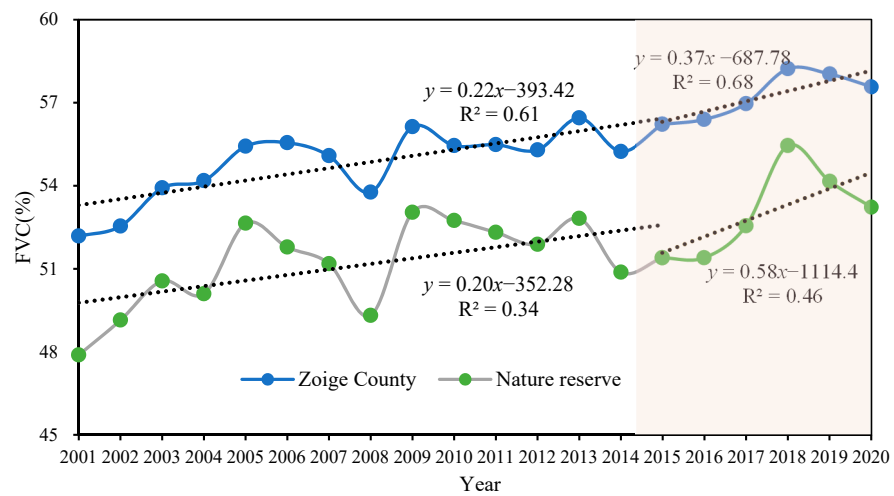


Figure 3. Interannual variation in fractional vegetation cover (FVC) in Zoige county and the nature reserve from 2001 to 2020.

It can be seen that the FVC of the Zoige Wetland National Nature Reserve also demonstrated an increasing trend, consistent with the changing trend of the whole county, and reflecting the overall improvement in vegetation growth. The mean FVC in the protected area was smaller than the average FVC of the whole county, mainly due to the existence of a forest ecosystem in the east of the county. However, from 2015 to 2020, the FVC in the reserve significantly improved, and was approximately 1.35-fold larger than the increase of the county value. This suggests stronger ecological resilience in the reserve.

From 2001 to 2020, the FVC in Zoige county increased at an annual rate of 0.25%; the FVC of 95.23% of the county increased, of which 63.6% of the area experienced significant increases (Figure 4). The rapidly increasing area was concentrated in the east, where forest and grassland met, and the nature reserve is located. Across the county, the area of FVC decrease accounted for 4.5%, mainly distributed in the northwest, where urban and rural land was concentrated. By comparing high-resolution remote-sensing images, some illegal facilities in the reserve were demolished (Figure 5).

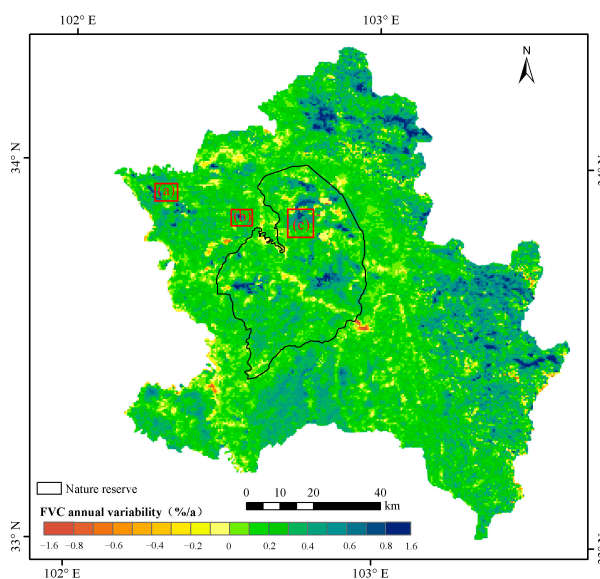


Figure 4. Cont.

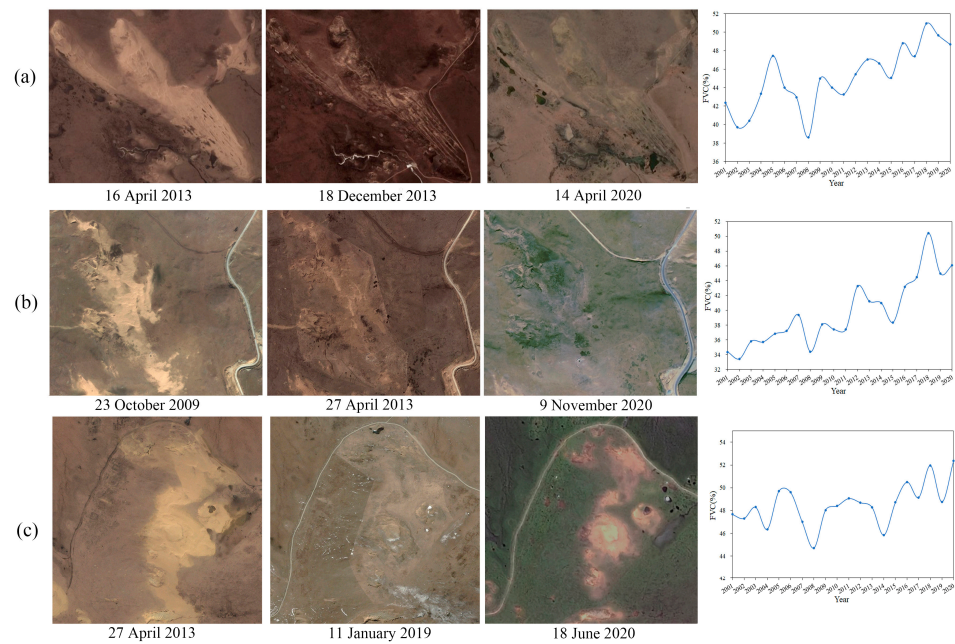


Figure 4. Changes in trend of fractional vegetation cover (FVC) in Zoige county from 2001 to 2020: (a–c) are the remote-sensing image comparison maps and vegetation coverage change time-series map of three typical ecological engineering implementation points. High-resolution remote-sensing images are from Google Earth and Chinese GF-1 satellites.



Figure 5. Comparison of remote-sensing images of demolition points of typical illegal facilities (high-resolution remote-sensing images from Chinese GF-1 and GF-2 satellites).

From 2015 to 2020, the rate of FVC increase escalated in both Zoige county and the reserve. The growth rate of the reserve (0.68% per year) was greater than that of the county as a whole (0.36%/a), reflecting the positive effects of targeted vegetation protection.

3.2. Water Body Change Characteristics

Remote-sensing data revealed that the water area of Zoige county in 2020 was 71.8 km², and mainly comprising the Yellow, Baihe, and Heihe Rivers in the west, along with the Huahu and Cuorewajian Lakes, and surrounding water bodies in the northwest.

The average water area of Zoige county from 2001 to 2020 was approximately 42.77 km². It exhibited an increasing trend. The water body area was lowest in 2002 (29.7 km²). In 2020, the water body area was approximately 32.66 km² larger than that in 2001, an increase of 83.44% (Figure 6). By comparing high-resolution remote-sensing images, we noted that the area of some water bodies in Zoige county has surged (Figure 7).

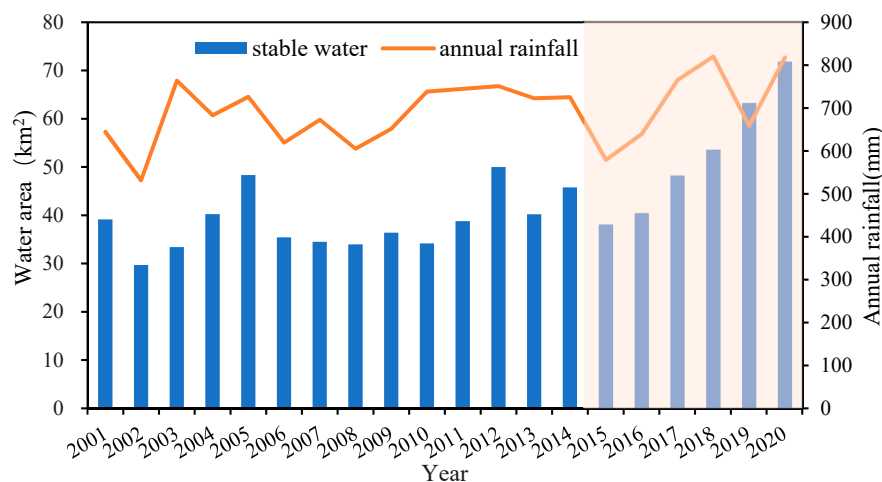


Figure 6. Changes in the stable water area in Zoige county from 2001 to 2020.

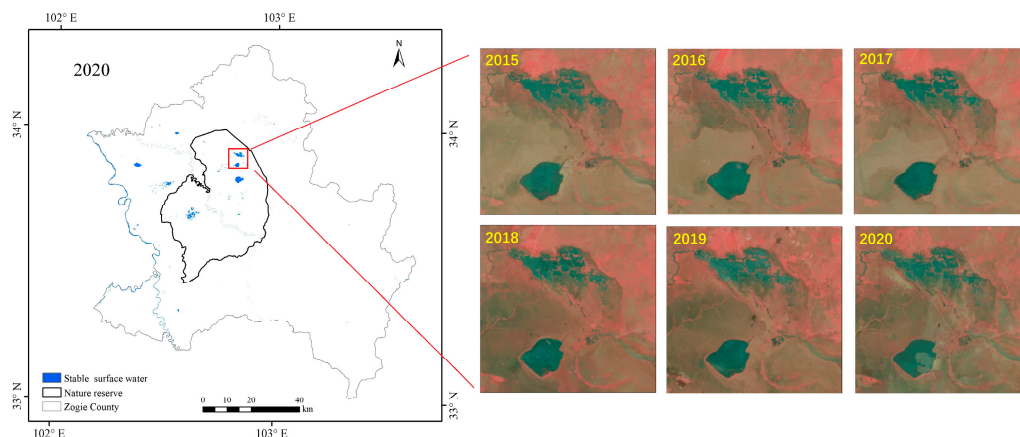


Figure 7. Spatial distributions of water area in Zoige county in 2020 and Landsat remote-sensing images of the Huahu Lake.

Viewed by stages, the water body area in Zoige county was basically stable from 2001 to 2015, and continued to increase after 2015. From 2015 to 2020, the county’s water body area rapidly increased, reaching nearly 1.83 times the level of early 2001.

3.3. Characteristics of Water Conservation Function

From 2016 to 2020, the mean annual water conservation capacity of Zoige county was approximately $21.2 \times 10^4 \text{ m}^3/\text{km}^2$, and high-value areas were mainly distributed in the southern herbaceous swamp and lake area and eastern mountainous forest area (Figure 8). The mean annual water conservation capacity in the Nature Reserve from 2016 to 2020 was $19 \times 10^4 \text{ m}^3/\text{km}^2$.

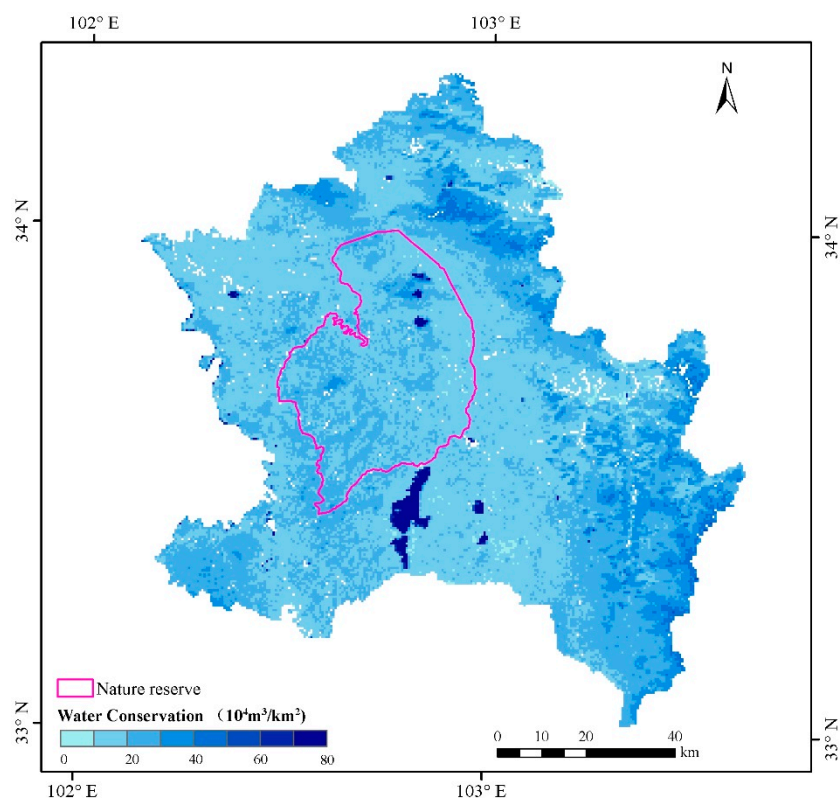


Figure 8. The mean value of water conservation in Zoige county (2016–2020).

From 2001 to 2020, the mean annual water conservation capacity of the county was $18.41 \times 10^4 \text{ m}^3/\text{km}^2$, and showed a decreasing and then increasing trend (Figure 9). Water conservation capacity in the county increased from $19.8 \times 10^4 \text{ m}^3/\text{km}^2$ in 2001–2005 to $21.2 \times 10^4 \text{ m}^3/\text{km}^2$ in 2015–2020, an increase of 15.23%.

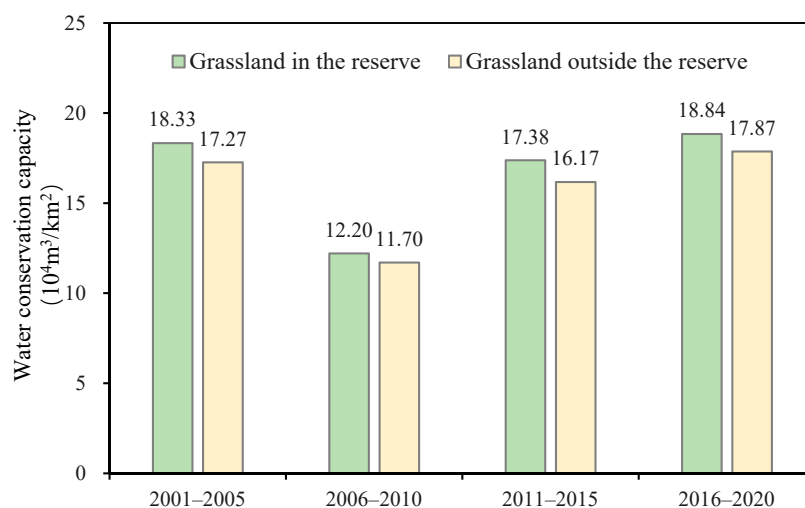


Figure 9. Annual change of water conservation in Zoige county from 2001 to 2020.

From 2001 to 2020, water conservation in Zoige county increased at a rate of $0.25 \times 10^4 \text{ m}^3/\text{km}^2/\text{year}$, and 84.55% of the region exhibited an increasing trend. Areas with the fastest growth rates were mainly located in the northern part of the reserve and the forested areas in the eastern part of Zoige county. Overall, water conservation in 15.02% of the county decreased, and the areas with the fastest decrease were mainly distributed in the west and south of Zoige county (Figure 9).

Between 2001 and 2020, the annual average water conservation of the nature reserve was $16.89 \times 10^4 \text{ m}^3/\text{km}^2$; water conservation of the reserve increased at a rate of approximately $0.2 \times 10^4 \text{ m}^3/\text{km}^2/\text{year}$, with 80.9% of the area experiencing an increasing trend. The reserve consisted of mainly grassland ecosystems. Although the average water conservation in the entire reserve was slightly lower than that in the whole county, the average water conservation in the grasslands of the reserve was about $1 \times 10^4 \text{ m}^3/\text{km}^2$ higher than that of the surrounding grasslands (Figure 10).

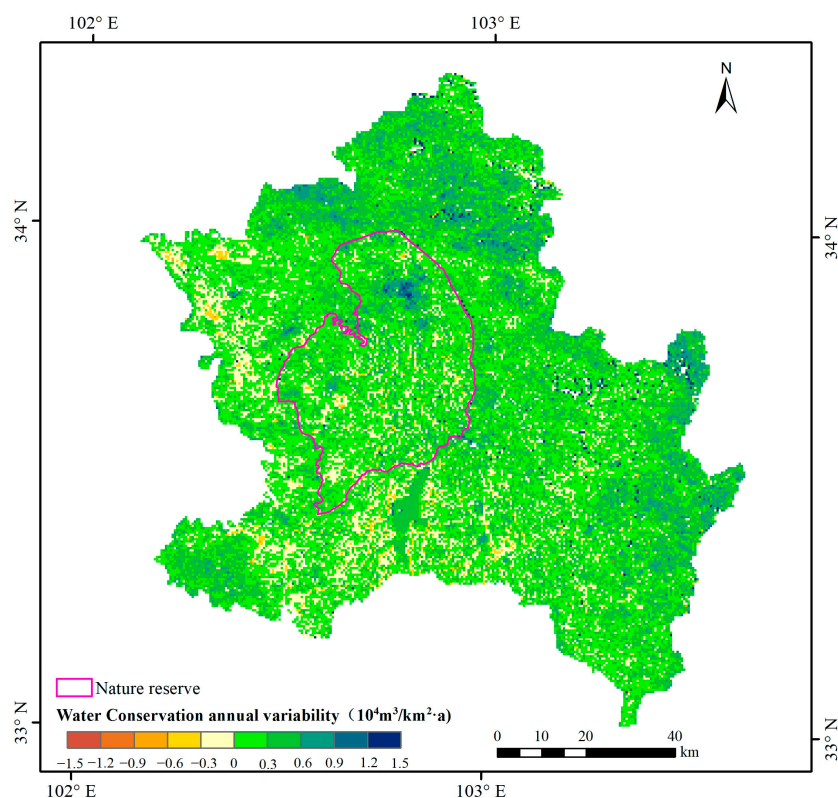


Figure 10. Variation trend in water conservation of Zoige county from 2001 to 2020.

4. Discussion

The purpose of this study was to make full use of satellite remote-sensing images with different resolutions to try to capture the changes in the ecosystem in Zoige from different scales, in order to corroborate changes in statistical analysis indicators and determine the intuitive characteristics of surface information. Furthermore, the objective of this study was also to analyze and evaluate the causes of ecosystem changes at the regional scale, and help us put forward specific and quantitative measures for regional ecological protection and restoration. Remote sensing has proven to be both feasible and effective. However, the existing indicators still require improvement.

The FVC describes key parameters of land surface vegetation, and reflects the structural characteristics of vegetation [30]. For grassland ecosystems, FVC is the basic index that reflects changes in ecological status. Here, we used FVC to monitor and evaluate the basic vegetation status of Zoige county. Furthermore, it was utilized to describe the regional ecological protection status by comparing high-resolution images of grassland and sand variations. However, FVC has obvious limitations in identifying the succession direction of the vegetation community. For example, FVC cannot directly reflect the characteristics of forage productivity, nor can it reflect the quantitative characteristics of dominant forage. Therefore, for future monitoring and evaluation of grassland ecosystem restoration, as well as for desertification control effectiveness analysis, it will be necessary to continuously carry out long-term tracking of ground communities in the Zoige area, especially in the

grassland ecosystem restoration area. Additionally, it is necessary to comprehensively evaluate the effectiveness of regional ecological protection in terms of quantity, productivity, and grassland quality.

Due to the influence of climate warming and humidification, glacier melting and surface runoff have increased to a certain extent, which has contributed to the increase in the area of regional lakes and other water bodies, and consequently to the amount of water conservation [35,41]. We used Landsat satellite imagery to extract the water body area with a spatial resolution of 30 m. However, water bodies of subpixel size are widely distributed in the peat swamp area, which is not only an important indicator of regional water conservation function, but also very important for climate change research, including regional greenhouse gas change monitoring [41]. Therefore, to carry out a more refined regional ecological function assessment of the Zoige wetland, it will be necessary to perform higher-resolution identification of water information. In the future, we will explore the driving effects of human activities and climate change on ecological conditions.

Water conservation is the dominant ecosystem function in the Zoige area. As an internationally important wetland, the Zoige wetland is also a habitat for rare species such as black-necked cranes, and the function of maintaining biodiversity is also worthy of attention. Therefore, in the future, we will also evaluate ecosystem protection effectiveness and develop technical methods for researching regional biodiversity based on satellite remote-sensing images [41].

5. Conclusions

From 2001 to 2020, the changes in vegetation and water bodies showed that the ecological status of Zoige improved, especially within the last five years (2015–2020). The vegetation coverage of the county showed an increasing trend; about 95.23% of the county experienced increasing vegetation coverage. During 2015–2020, the growth rate of vegetation coverage was 1.64 times higher than that of the previous 15 years (2001–2015). In the last five years, the water area increased by 77.35%, which is the fastest period of increase in the past two decades.

Local land desertification control, wetland restoration, restrictions on illegal construction in nature reserves, facility demolition, and other protective measures not only reflect the local government's determination and willingness to protect the ecological environment, but also to improve the quality of the environment. Based on an interannual comparison of high-resolution satellite images, some land desertification control areas in the county have been restored to green. For example, the vegetation coverage of typical patches for desertification control had increased by about 5–10% since the implementation of the project in 2016. Some dried lakes and marshes have also been significantly restored. For example, multiphase remote-sensing images showed that the water body of Huahu Lake in the reserve has increased, and the surrounding land has become more swampy.

Nature reserves generally represent areas with good ecological background and fragile ecology. Driven by regional ecological protection policies, the protection effects of nature reserves will be more prominent and direct (for example, faster vegetation restoration, priority of water body restoration, greater force of human interference reduction measures, etc.) In addition, nature reserves can play a leading and exemplary role in the protection of the overall ecological function of the region. Taking the water conservation function of grassland ecosystem as an example, the amount of water conservation within the nature reserve was about $1 \times 10^4 \text{ m}^3/\text{km}^2$ higher than that of the surrounding grasslands.

In the future, with the continuous enrichment in satellite remote-sensing data sources, especially with the increase in high-resolution images, it will be possible to extract high-spatial resolution and long time series of vegetation, water and other information, which will be very useful to improving the accuracy of regional ecological protection and assessment, and even replace most of the ground investigation and engineering implementation assessment tasks. Information pertaining to regional ecological function changes will be further refined with this new technology.

Author Contributions: Conceptualization, P.H. and J.Z.; methodology, Y.Z.; formal analysis, J.Z. and H.-F.G.; data curation, D.-D.J. and Y.C.; writing—original draft preparation, D.-D.J.; writing—review and editing, D.-D.J., J.Z. and P.H.; funding acquisition, P.H. All authors have read and agreed to the published version of the manuscript.

Funding: This research was funded by National Key R&D Program of China (grant number 2021YFF0703903) and Major Projects of High-Resolution Earth Observation Systems of National Science and Technology (grant number 05-Y30B01-9001-19/20-4).

Institutional Review Board Statement: Not applicable.

Data Availability Statement: Not applicable.

Acknowledgments: Thanks to the local environmental protection bureau for its help with the field investigation.

Conflicts of Interest: The authors declare no conflict of interest.

References

- Zakharov, I.; Kapfer, M.; Hornung, J.; Kohlsmith, S.; Puestow, T.; Howell, M.; Henschel, M.D. Retrieval of Surface Soil Moisture from Sentinel-1 Time Series for Reclamation of Wetland Sites. *IEEE J. Sel. Top. Appl. Earth Obs. Remote Sens.* **2020**, *13*, 3569–3578. [\[CrossRef\]](#)
- Mleczko, M.; Mroz, M.; Fitzryk, M. Riparian wetland mapping and inundation monitoring using amplitude and bistatic coherence data from the tandem-x mission. *IEEE J. Sel. Top. Appl. Earth Obs. Remote Sens.* **2021**, *14*, 2432–2444. [\[CrossRef\]](#)
- Guo, M.; Li, J.; Sheng, C.-L.; Xu, J.-W.; Wu, L. A review of wetland remote sensing. *Sensors* **2017**, *17*, 777. [\[CrossRef\]](#) [\[PubMed\]](#)
- Hu, S.; Niu, Z.; Chen, Y. Global Wetland Datasets: A Review. *Wetlands* **2017**, *37*, 807–817. [\[CrossRef\]](#)
- Jiang, N.; Wang, Y.-F.; Dong, X.-Z. Methanol as the Primary Methanogenic and Acetogenic Precursor in the Cold Zoige Wetland at Tibetan Plateau. *Microb. Ecol.* **2010**, *60*, 206–213. [\[CrossRef\]](#)
- Li, M.; Xu, R.; Huang, W.; Sun, H.; Luo, L. A study on the effects of the surrounding faults on water loss in the Zoige Wetland, China. *J. Mt. Sci.* **2011**, *8*, 518–524. [\[CrossRef\]](#)
- Tan, Y.-Y.; Wang, X.; Li, C.-H.; Cai, Y.-P.; Yang, Z.-F.; Wang, Y.-L. Estimation of ecological flow requirement in Zoige Alpine Wetland of Southwest China. *Environ. Earth Sci.* **2012**, *66*, 1525–1533. [\[CrossRef\]](#)
- Guo, B.; Wang, S.; Wang, M.-T. Spatio-temporal variation of NPP from 1999 to 2015 in Zoige grassland wetland. *Chin. J. Appl. Ecol.* **2020**, *31*, 424–432.
- Yu, H.; Luedeling, E.; Xu, J. Winter and spring warming result in delayed spring phenology on the Tibetan Plateau. *Proc. Natl. Acad. Sci. USA* **2010**, *107*, 22151–22156. [\[CrossRef\]](#)
- Fei, S.-M.; Cui, L.-J.; He, Y.-P.; Chen, X.-M.; Jiang, J.-M. A background study of the wetland ecosystem research station in the Ruergai Plateau. *J. Sichuan For. Sci. Technol.* **2006**, *27*, 21–29.
- Wang, R.; He, M.; Niu, Z.-G. Responses of Alpine Wetlands to Climate Changes on the Qinghai-Tibetan Plateau Based on Remote Sensing. *Chin. Geogr. Sci.* **2020**, *30*, 189–201. [\[CrossRef\]](#)
- Kang, X.-M.; Hao, Y.-B.; Cui, X.-Y.; Chen, H.; Huang, S.-X.; Du, Y.-G.; Li, W.; Kardol, P.; Xiao, X.-M.; Cui, L.-J. Variability and Changes in Climate, Phenology, and Gross Primary Production of an Alpine Wetland Ecosystem. *Remote Sens.* **2016**, *8*, 391. [\[CrossRef\]](#)
- Jin, X.-Y.; Qiang, H.-F.; Zhao, L.; Jiang, S.-Z.; Cui, N.-B.; Cao, Y.; Feng, Y. SPEI-based analysis of spatio-temporal variation characteristics for annual and seasonal drought in the Zoige Wetland, Southwest China from 1961 to 2016. *Theor. Appl. Climatol.* **2020**, *139*, 711–725. [\[CrossRef\]](#)
- Xia, H.-M.; Zhao, W.; Li, A.-N.; Bian, J.H.; Zhang, Z.-J. Subpixel Inundation Mapping Using Landsat-8 OLI and UAV Data for a Wetland Region on the Zoige Plateau, China. *Remote Sens.* **2017**, *9*, 31. [\[CrossRef\]](#)
- Shen, G.-Y.; Yang, X.-C.; Jin, Y.-X.; Xu, B.-Z.; Zhou, Q.-B. Remote sensing and evaluation of the wetland ecological degradation process of the Zoige Plateau Wetland in China. *Ecol. Indic.* **2019**, *104*, 48–58. [\[CrossRef\]](#)
- Kuang, Q.; Yuan, Q.-Z.; Han, J.-C.; Leng, R.; Wang, Y.-S.; Zhu, K.-H.; Lin, S.; Ren, P. A remote sensing monitoring method for alpine grasslands desertification in the eastern Qinghai-Tibetan Plateau. *J. Mt. Sci.* **2020**, *17*, 1423–1437. [\[CrossRef\]](#)
- Fei, Y.; Wang, J.-Y.; Wang, Z.-G. Dynamic changes of land desertification in Zoige Plateau. *J. Arid Land Resour. Environ.* **2019**, *33*, 146–152.
- Ma, K.; Zhang, Y.; Tang, S.-X.; Liu, J.-G. Spatial distribution of soil organic carbon in the Zoige Alpine Wetland, Northeastern Qinghai-Tibet Plateau. *Catena* **2016**, *144*, 102–108. [\[CrossRef\]](#)
- Ma, K.; Liu, J.-G.; Balkovič, J.; Skalský, R.; Azevedo, L.B.; Kraxner, F. Changes in soil organic carbon stocks of wetlands on China's Zoige plateau from 1980 to 2010. *Ecol. Model.* **2016**, *327*, 18–28. [\[CrossRef\]](#)
- Li, J.-C.; Wang, W.-L.; Hu, G.-Y.; Wei, Z.-H. Changes in ecosystem service values in Zoige Plateau, China. *Agr. Ecosyst. Environ.* **2010**, *139*, 766–770. [\[CrossRef\]](#)

21. Wu, C.-Y.; Chen, W.; Cao, C.-X.; Tian, R.; Liu, D.; Bao, D.-M. Diagnosis of Wetland Ecosystem Health in the Zoige Wetland, Sichuan of China. *Wetlands* **2018**, *38*, 469–484. [[CrossRef](#)]
22. Lu, F.; Hu, H.-F.; Sun, W.-J.; Zhu, J.-J.; Liu, G.-B.; Zhou, W.-M.; Zhang, Q.-F.; Shi, P.-L.; Liu, X.-O.; Wu, X.; et al. Effects of national ecological restoration projects on carbon sequestration in China from 2001 to 2010. *Proc. Natl. Acad. Sci. USA* **2018**, *115*, 4039–4044. [[CrossRef](#)] [[PubMed](#)]
23. Zhang, X.; Wang, J.; Gao, Y.; Wang, L. Variations and controlling factors of vegetation dynamics on the Qingzang Plateau of China over the recent 20 years. *Geogr. Sustain.* **2021**, *2*, 74–85. [[CrossRef](#)]
24. Gao, J.-X.; Xu, M.-J.; Zou, C.-X. Development Achievement of Natural Conservation in 70 Years of New China. *Chin. J. Environ. Manag.* **2019**, *11*, 25–29.
25. Kuang, Q. Study on the Coupling Relationship between Development of Alpine Animal Husbandry and Restoration of Sandy Grassland in Northwest Sichuan: A Case Study of Zoige. Master's Thesis, Sichuan Normal University, Chengdu, China, 2020.
26. Dong, S.-L.; Zhang, T.-S. Ecological status quo and benefit analysis of protection measures in Zoige County. *Prataculture Anim. Husb.* **2012**, *8*, 30–32 + 53.
27. Hou, P.; Zhai, J.; Cao, W.; Yang, M.; Cai, M.-Y.; Li, J. Evaluation on ecosystem changes and protection of the national key ecological function zones in mountainous areas of central Hainan Island. *Acta Geogr. Sin.* **2018**, *73*, 429–441.
28. Gao, Y.-P.; Zhang, X.-X.; Fang, Y.; Zhang, X.; Guo, J.-B. Landscape fragmentation and wetland restoration priority in Zoige County of Sichuan Province of China. *J. China Agric. Univ.* **2019**, *24*, 145–158.
29. Cui, Y.; Zhang, X.-X.; Zhang, X.; Fang, Y.; Guo, C.-Q. Hydrological and geomorphologic ecological threshold of steady-state transformation of wetland in Zoige County. *Acta. Ecol. Sin.* **2020**, *40*, 8794–8804. [[CrossRef](#)]
30. Jiapaer, G.-L.; Chen, X.; Bao, A. A comparison of methods for estimating fractional vegetation cover in arid regions. *Agr. For. Meteorol.* **2011**, *151*, 1698–1710. [[CrossRef](#)]
31. Gutman, G.; Ignatov, A. The derivation of the green vegetation fraction from NOAA/AVHRR data for use in numerical weather prediction models. *Int. J. Remote Sens.* **1998**, *19*, 1533–1543. [[CrossRef](#)]
32. Ivits, E.; Cherlet, M.; Sommer, S.; Mehl, W. Addressing the complexity in non-linear evolution of vegetation phenological change with time-series of remote sensing images. *Ecol. Indic.* **2013**, *26*, 49–60. [[CrossRef](#)]
33. Song, W.-J.; Mu, X.-H.; Ruan, G.-Y.; Gao, Z. Estimating fractional vegetation cover and the vegetation index of bare soil and highly dense vegetation with a physically based method. *Int. J. Appl. Earth Obs.* **2017**, *58*, 168–176. [[CrossRef](#)]
34. Gao, J.-X.; Wang, Y.-C.; Hou, P.; Wan, H.-W.; Zhang, W.-G. Temporal and spatial variation characteristics of land surface water area in the Yellow River basin in recent 20 years. *J. Hydraul. Eng.* **2020**, *51*, 1157–1164. [[CrossRef](#)]
35. Pekel, J.F.; Cottam, A.; Gorelick, N.; Belward, A.S. High-resolution mapping of global surface water and its long-term changes. *Nature* **2016**, *540*, 418–422. [[CrossRef](#)] [[PubMed](#)]
36. Gong, S.; Yang, X.; Zheng, H.; Xiao, Y.; Ouyang, Z. Spatial patterns of ecosystem water conservation in China and its impact factors analysis. *Acta Ecol. Sin.* **2017**, *37*, 2455–2462. [[CrossRef](#)]
37. Wu, B.-F.; Yuan, Q.-Z.; Yan, C.-Z.; Wang, Z.-M.; Yu, X.-F.; Li, A.-N.; Ma, R.-H.; Huang, J.-L.; Chen, J.-S.; Chang, C.; et al. Land cover changes of China from 2000 to 2010. *Quat. Sci.* **2014**, *34*, 723–731.
38. Wu, D.-H.; Wu, H.; Zhao, X.; Zhou, T.; Tang, B.-J.; Zhao, W.-Q.; Jia, K. Evaluation of spatiotemporal variations of global fractional vegetation cover based on GIMMS NDVI data from 1982 to 2011. *Remote Sens.* **2014**, *6*, 4217–4239. [[CrossRef](#)]
39. Mann, H.-B. Nonparametric tests against trend. *Econometrica* **1945**, *13*, 245–259. [[CrossRef](#)]
40. Kendall, M.-G. *Rank Correlation Methods*; Griffin: London, UK, 1948.
41. Woolway, R.I.; Kraemer, B.M.; Lenters, J.D.; Merchant, C.J.; O'Reilly, C.M.; Sharma, S. Global lake responses to climate change. *Nat. Rev. Earth Environ.* **2020**, *1*, 388–403. [[CrossRef](#)]